Experimental Validation of the linear drive train for a Total Artificial Heart System

André Pohlmann [1], Marc Leßmann [1], Andreas Fritschi [2], Thomas Finocchiaro [2], Ulrich Steinseifer [2] and Kay Hameyer [1]

[1]Institute of Electrical Machines, RWTH Aachen University, Schinkelstr. 4, D-52062 Aachen Germany
[2]Chair of Applied Medical Engineering, RWTH Aachen University, Pauwelsstr. 20, D-52074 Aachen Germany
email: andre.pohlmann@iem.rwth-aachen.de

ABSTRACT

In industrialized countries cardiovascular diseases are the major cause of death. Beside heart transplants, which are a limited option due to the limited number of available human donor hearts, Total Artificial Hearts (TAHs) are the only therapy available for some patients with terminal heart diseases. For various reasons a total implantable artificial heart is desirable, but also sets restrictions in terms of weight and dimensions due to the limited space in the human thorax. Therefore a precise requirement profile is needed for the drive design to provide sufficient force for the blood pump and to avoid oversizing of the drive and to prevent blood damage by overheating.

1 INTRODUCTION

According to the World Health Organization (WHO) [1] cardiovascular diseases are the major cause of death in industrialized countries. Currently there are only two therapy possibilities for the treatment of terminal heart diseases, which are transplantation of donor hearts or implantation of artificial hearts, which can either support or replace the human heart. In the United States of America the demand for donor hearts has doubled, while the number of available donor organs is decreasing [2]. This example shows that donor heart transplantation is a limited therapy option.

On the other hand, there is only one clinical approved Total Artificial Heart system, which is called CardioWest [3]. This TAH meets the implantation constraints in terms of weight and dimensions and is able to take over the heart function. As this blood pump is actuated with compressed air, it requires drivelines penetrating the human abdominal wall, increasing the risk of infections. Further the size and the weight of the outside compressor reduces the quality of life for the patient.

In order to avoid these disadvantages an electrically driven and totally implantable blood pump in combination with a wireless power transmission system is desirable. An example of such a system is presented in Fig. 1. An external battery is connected to a transcutaneous energy transfer (TET) system. The TET system is based on an inductive coupling between an external primary and an implanted secondary coil [4], charging internal buffer batteries and supplying the drive controller of the electrical actuated TAH.

After implanting a TAH a maintenance of the system is impossible. Additionally a long durability is desired because of the severe implantation surgery, yielding a long recovery duration of the patient. Therefore the TAH ReinHeart, shown in Fig. 2, is actuated by an electric linear drive, to avoid as many wear prone components such as gears or transducers as possible. The drive is located betweeen the two blood chambers, which are evacuated by two pusher plates. In this way a pulsatile blood flow is induced, regulated by the inlet and outlet valves. Each chamber has a capacity of $65\,\mathrm{ml}$. When expecting flow losses, in theory $100\,\mathrm{bpm}$ (beats per minute) yield a blood flow of $6\,\mathrm{l}$ of blood per minute. The specifications for the drive are given in the following sections.

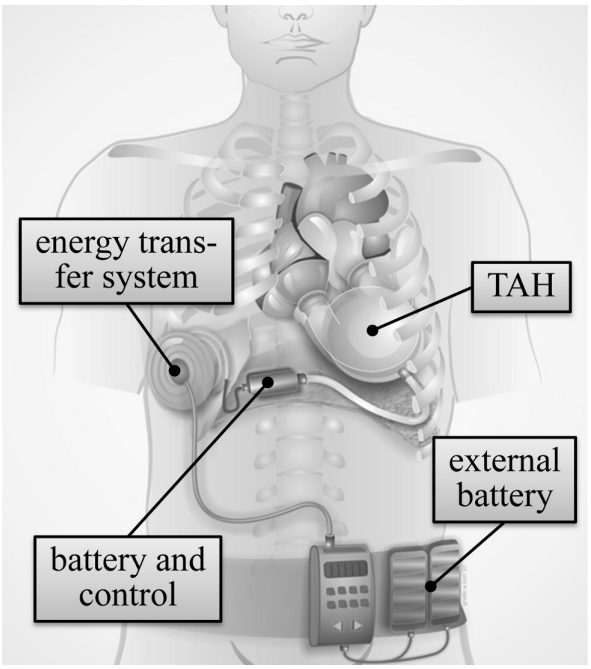

Figure 1: Total Artificial Heart system.

2 FORCE VS. DISPLACEMENT CHARACTERISTIC

For the implantation of an artificial heart, the constraints listed in [5] have to be meet in order to ensure a sufficient perfusion of the human body without blood or tissuer damage. The maximum allowable weight of $900\,\mathrm{g}$ and dimensions of $85\,\mathrm{mm}$ in diameter and $95\,\mathrm{mm}$ in lenght for the TAH design to meet the given constraints.

For electrical drives the limiting factor for miniaturisation are cooling issues in general. In case of a TAH the cooling medium is blood, which must not exceed a

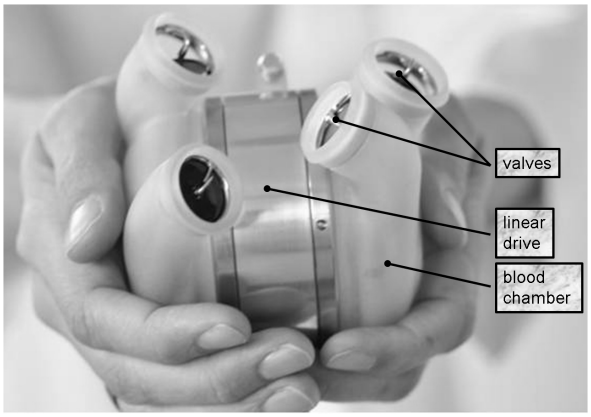

Figure 2: Total Artificial Heart ReinHeart.

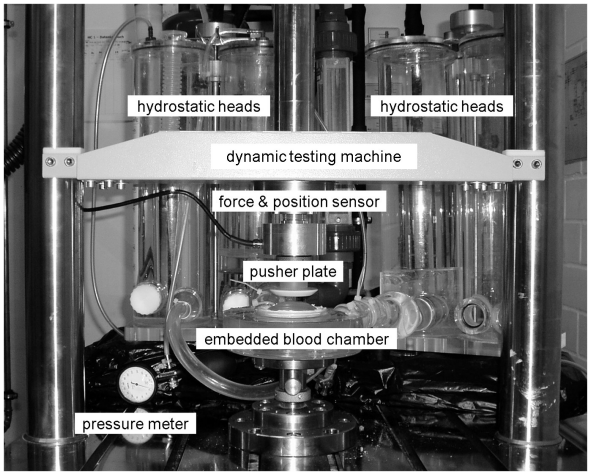

Figure 3: Measurement of force vs. displacement characteristic.

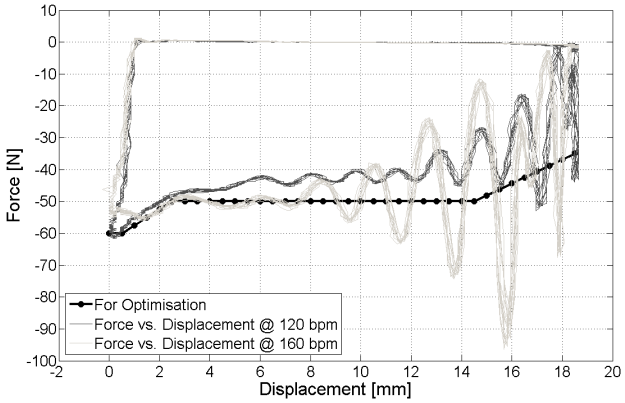

Figure 4: Force vs. Displacement of Systemic Blood Circuit.

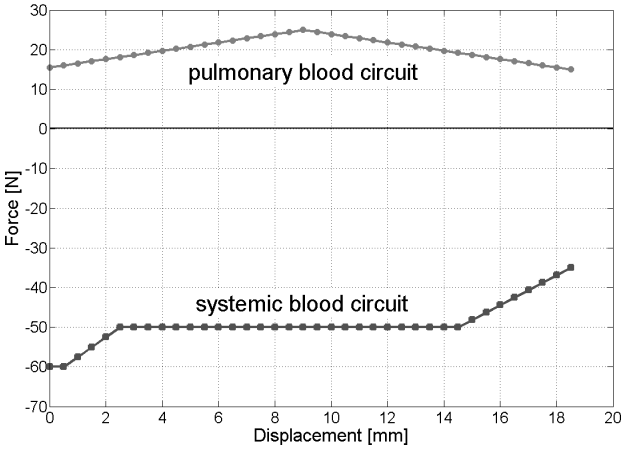

Figure 5: Force vs. Displacement characteristic for drive design.

temperature of $42\,\mathrm{C}^\circ$ to avoid its decay by denaturation. Therefore the electrical losses of the drive are limited to a maximum of $20\,\mathrm{W}$. Additionally this limit is required to allow for the operation of a TET system. These factors demand a precise knowledge of the required forces for the blood pump to be able to replace the human heart. In [6] a force vs. displacement characteristic was deduced from the occuring pressures at the beginning and the end of the systolic phase of the human heart for the systemic and pulmonary blood circuit. As this approach does not consider the blood pump design, the test bench in Fig. 3 is set up to obtain a specific characteristic for the drive design.

A dynamic tensile testing machine replaces the linear drive in this assembly and moves a pusher plate, which evacuates a blood chamber. The physical constraints of the human body are simulated with a circulatory mock loop. It consists of two hydrostatic heads, representing the pressures in the systemic and pulmonary blood circuit. Further it provides compliances to imitate the elasticity of the arterial vessels as well as resistances for considering the pressure drop in the capilaries. During pumping operation, the required forces for evacuating the blood chamber, the position of the pusher plate and the resulting flow are measured, while the pumping frequency f_{pump} is given by the testing machine controller. For the measurements a fluid mixture of $60\,\%$ water and $40\,\%$ is applied, which viscosity is similar to the one of blood.

Figure 4 represents the force vs. displacement characteristics for the systemic blood circuit, which has a medium aortic pressure of $100\,\mathrm{mmHg}$. For a pumping frequency of $120\,\mathrm{bpm}$ a perfusion of about $6\,\mathrm{l}$ of blood per minute is achieved. At a displacement of $0\,\mathrm{mm}$ the blood chamber is completely evacuated and the maximum absolut force of $60\,\mathrm{N}$ is required for this frequency. This is due to the systolic pressure of $120\,\mathrm{mmHg}$ and the maximum elongation of the blood chamber diaphragm. When the pusher plate is moving upwards the fluid fills the blood chamber again. In this phase the pusher plate has no contact to the diaphragm of the blood chamber and the resulting pumping force is $0\,\mathrm{N}$. At a displacement of $18.5\,\mathrm{mm}$ the moving direction turns back and the pusher plate is clashing against the diaphragm. This results in force oscillations at the beginning of the systolic phase. The magnitude of the oscillations rises with the increased pumping frequency and reaches its peak value of $-95\,\mathrm{N}$ at a displacement of $16\,\mathrm{mm}$ and a frequency f_{pump} of $160\,\mathrm{bpm}$. With the linear drive proposed in [6], this force can only be generated when exceeding the loss limit of $20\,\mathrm{W}$. For this reason the graph for the drive design takes the average forces in the range of the

oscilations and the maximum forces at the end of the systolic phase into account.
The absolut values of the required forces to achieve a sufficient perfusion of the pulmonary blood circuit are lower when compared to the systemic blood circuit, due to the lower medium pressure of $27\,\mathrm{mmHg}$ (s. Fig 5). In reality this medium pressure is even lower, but can not be measured due to the adjustable pressure range of the test bench. According to

$$F_{max} = m \cdot a_{max} \quad , \tag{1}$$

the peak force F_{max} is generated, when the acceleration a reaches its maximum value and the mass m is constant. As the pusher plates are driven with a sinusoidal movement the maximum acceleration a_{max} occurs in the inflexion point of the movement, which is located at a displacement d of $9.25\,\mathrm{mm}$. Under perfect conditions the generel shape of the design characteristic for the systemic and pulmonary blood circuit should be similar. But regarding the higher resulting pressures in the systemic circuit, the flow losses are significantly higher. Due to these losses the desired blood flow of $6\,\mathrm{l}$ of blood per minute is not achieved until a frequency f_{pump} of $120\,\mathrm{bpm}$ exceeding the theoretical calculated frequency of $100\,\mathrm{bpm}$.

3 DRIVE DESIGN

The general design of the linear drive is shown in Fig. 6. For the first design the maximum allowable space is used, resulting in an outer drive diamter of $85\,\mathrm{mm}$ and a maximum length composed by the height of the static drive part ($16.5\,\mathrm{mm}$) and the stroke length of $18.5\,\mathrm{mm}$. This results in a blood chamber height of $30\,\mathrm{mm}$. The drive is excited by an inner and outer permanent magnet ring, made of neodymium iron boron (NdFeB). Due to manufactoring the remanent induction B_r of the inner ring is higher than for the outer ring with values of $1.45\,\mathrm{T}$ and $1.4\,\mathrm{T}$ at room temperature. According to

$$B_r = B_r(20\,^\circ) \cdot (1 - \alpha \cdot \Delta T) \tag{2}$$

$$\alpha = 0.12\,\frac{\%}{\mathrm{K}}, \Delta T = 30\,\mathrm{K}$$

the remanent induction is further reduced, when assuming a temperature of $50\,^\circ\mathrm{C}$ inside the magnets during TAH operation. The resulting flux density is concentrated inside the air gap by the pole shoes above and beyond the magnet rings. They are made of an iron vanadium cobalt alloy with a saturation induction of up to $2.4\,\mathrm{T}$. The mover consists of four seperately supplyable coils to allow for a position dependent coil supply.

Basicly the drive is actuated by a Lorentzforce F_L, generated by a flux density B and a dc current I injected into the coil windings with an active wire length l:

$$\vec{F}_L = I \cdot (\vec{l} \times \vec{B}) \quad . \tag{3}$$

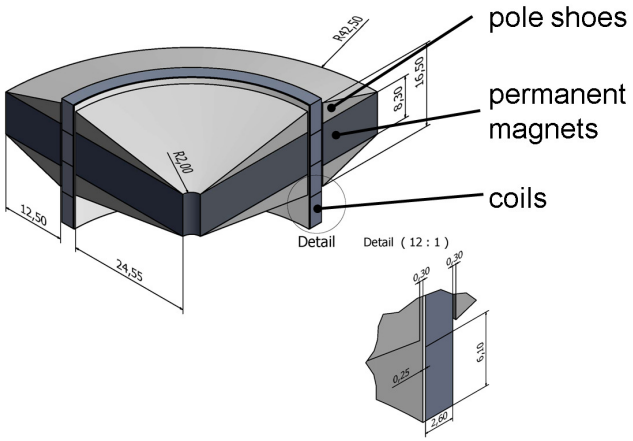

Figure 6: CAD drawing of TAH ReinHeart.

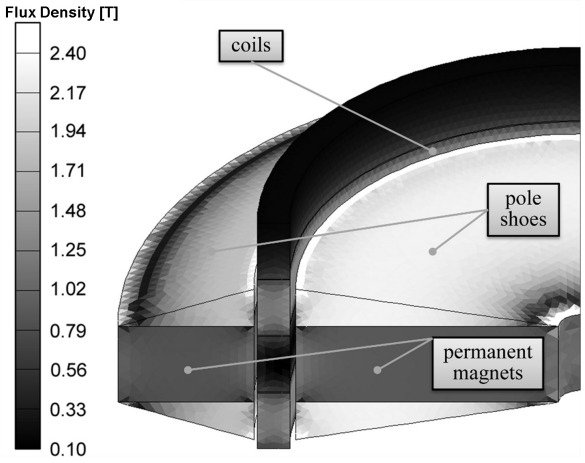

Figure 7: Flux density distribution in the drive of the TAH ReinHeart.

In this design the flux density B is only generated by the permanent magnet rings. This statement is justified, because even for a high heart beat rate of $180\,\mathrm{bpm}$ the resulting frequency is only $3\,\mathrm{Hz}$. Further, the air gap thickness amounts to about $4\,\mathrm{mm}$. Therefore a significant amount of stray flux is expected. Relying on these facts static and non linear Finite Element (FE) simulations are applied to determine the flux density distribution inside the drive.
The flux density distribution of the drive design is shown in Fig. 7. As expected the flux is concentrated inside the air gap in the area of the pole shoes, but also the stray flux is partially penetrating the coils. In this position two coils are perfectly alligned to the pole shoes and the maximum flux density, yielding high forces at low losses, which is explained in the following. Therefore this position is defined to be $0\,\mathrm{mm}$ in accordance to Fig. 5.

After calculation of the flux density distribution and a constant wire length l the only remaining value for solving equation 3 is the coil supply I_N of each coil, resulting in position dependent copper losses:

$$P_{sum}(x) = \sum_{n=1}^{4} I_n^2(x) \cdot R \quad , \tag{4}$$

In order to achieve a sufficient perfusion of the human body, the drive has to provide the force displacement characteristic measured in Fig. 5. As the required forces are known, a calculation chain, based on a combination of FE-simulations and analytical equations, introduced in [7], is applied to optimize the current supply and to reduce the resulting electric losses, which finally sum up to 8 W for this drive design.

If all coils are supplied with the same dc current $I_n(x)$, the generated force of each coil $F_n(x)$ is proportional to the average radial amount of flux density $\overline{B}_{r,n}(x)$, penetrating each coil at a given axial displacement x. Therefore, the ratio of the average flux density $\overline{B}_{r,n}(x)$ penetrating one coil to the average flux density $\overline{B}_r(x)$ penetrating all coils can be determined with the current factors $k_I(x)$ for each displacement.

$$k_{I,n}(x) = \frac{\overline{B}_{r,n}(x)}{\sum_{n=1}^{4} |\overline{B}_{r,n}(x)|} \quad . \tag{5}$$

As the allowable ohmic losses are limited, the coil currents are limited as well. In order to achieve a maximized forces generation of all coils under the constraint that the sum of their current supplies $I_{sum}(x)$ is limited, all coils should be supplied according to their currentfactor $k_{I,n}$.

$$I_n(x) = k_{I,n}(x) \cdot I_{sum}(x) \tag{6}$$

The required force $F_r(x)$, which is obtained from the predefined force displacement curve, Fig. 5, has to be provided by all four coils.

$$F_r(x) = \sum_{n=1}^{4} I_n(x) \cdot l \cdot \overline{B}_{r,n}(x) \quad . \tag{7}$$

When inserting equation 6 in equation 7 and transforming the result to

$$I_{sum}(x) = \frac{F_r(x)}{\sum_{n=1}^{4} \overline{B}_{r,n}(x) \cdot k_{I,n}(x) \cdot l} \quad , \tag{8}$$

the coil supply to generate the required forces can be determined. Finally, the resulting position dependent ohmic losses $P_{sum}(x)$ are determined by accumulating the losses of each coil, which are calculated by multiplying the square of the coil's current $I_n(x)$ with its resistance R.

To compute the average losses during one beat cycle, the maximum axial displacement of the pusher plates of $18.5\,\mathrm{mm}$ is devided into segments with a length of $0.5\,\mathrm{mm}$:

$$x_m = m \cdot 0.5\,\mathrm{mm} \quad m = 0, ...37 \quad . \tag{9}$$

For each of these m segments the delay time t_m of the pusher plates within each segment is calculated, based on the assumption of a sinusoidal movement of the pusher plates:

$$t_m = \frac{\arcsin(\frac{x_{m+1} - 9.25\,\mathrm{mm}}{9.25\,\mathrm{mm}}) - \arcsin(\frac{x_m - 9.25\,\mathrm{mm}}{9.25\,\mathrm{mm}})}{2 \cdot \pi \cdot f} \quad . \tag{10}$$

Finally, the position dependent losses are weighted with the time factor t_m for the calculation of the average losses during one beat cycle: As the delay time t_m differs for each displacement due to the sinusoidal movement, the position dependent losses are weighted with t_m. By multiplying the weighted losses with the pumping frequency f the average losses $P_{sum}(x)$ are determined

$$P_{sum}(x) = f \cdot \sum_{m=0}^{36} P_{sum,fw/bw}(x_m) \cdot t_m \quad . \tag{11}$$

The medium pressure of the polmunary blood circuit ($27\,\mathrm{mmHg}$) is lower than in the arterial blood circuit ($100\,\mathrm{mmHg}$). Therefore the required forces and the resulting losses are lower in this case as well. For this reason the average electric losses $P_{sum}(x)$ are the sum of the resulting losses when evacuating the arterial blood chamber ($P_{sum,fw}$) and the pulmonary blood chamber ($P_{sum,bw}$).

4 VALIDATION OF THE DRIVE DESIGN

The designed drive was constructiveley integrated into a TAH with the pump unit, housing and further accessories such as sensors or the bearing. Then the prototype was connected to a circulatory mock loop, similar to the one used for the measurement of the force vs. displacement characteristic. As seen in Fig. 8, the flow rate, the pressures for the systolic and diastolic phase as well as the temperature of the fluid were measured to monitor the adjusted physical conditions. Additionally the electrical input power and current are measured for the converter and the drive. Before the resistances of the coils and the lead cables were measured under steady state conditions. Therefore the copper losses can be calculated by applying the equation

$$P_{cu} = I_{rms}^2 \cdot R \tag{12}$$

yielding losses of $8.3\,\mathrm{W}$ in the coils and $3.9\,\mathrm{W}$ in the lead cables. By subtracting these losses from the active power, the mechanical output power of $3.5\,\mathrm{W}$ remains. When comparing the measured copper losses of the coils with the simulated ones, which amount to $8\,\mathrm{W}$, the difference is in the range of $4\,\%$. This shows a good agreement between simulation and measurement, even when considering that the simulation is based on worst case conditions. On the way to a clinical approved TAH in-vivo test are required to validate it in the living organism. Therefor the prototype is implanted in a calf (s. Fig. 9), which anatomy

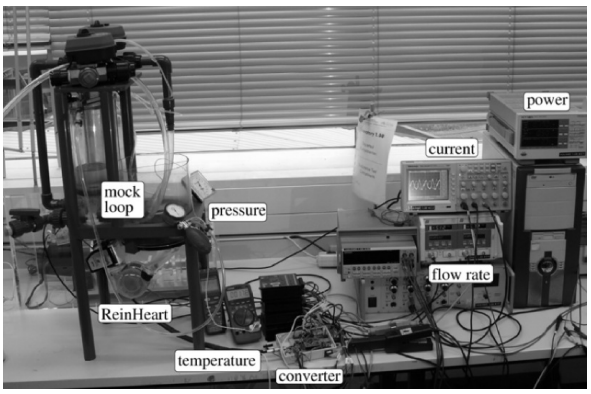

Figure 8: In vitro validation of the TAH ReinHeart.

Figure 9: TAH ReinHeart implanted in a calf.

is comparable to the human body, to prove its concepts under realistic condions.

For the validation and evaluation characeteristic values such as perfusion, pumping frequency, systolic and diastolic pressures or electrical input power are measured. As the right pusher plate is close to the coils, it is exspected to be one of the hot spots of the drive. Due to construction reasons only thermal indicators are applied to measure the maximum temperature. During several hours in-vivo tests the TAH provided a sufficient perfusion without overheating of the blood. Further, the blood samples taken during the tests showed no sign of damage. Therefore the TAH as well as the drive design is verified.

5 Conclusions

This paper explained the reasons for the development of TAH systems, which are mainly the insufficient number of available donor hearts for the treatment of patients, suffering from cardiovascular diseases. The only clinical approved TAH system CardioWest has limitations in terms of infection risks and quality of life, which might be solved by an electrical driven TAH system powered via a TET system. In order to avoid an oversizing a specific force vs. displacement characteristic to obtain precise constraints for the drive design of the TAH ReinHeart. The linear drive, which is based on a flux concentrating concept, reduces the amount of wear prone components to a minimum. Therefore a long durability is expected, but not proved in vivo yet.

Before dimensioning the drive an optimized current supply of the coils is determined by applying FEM simulations and analytical equations. Together with the obtained force vs. displacement characteristic, the resulting copper losses can be calculated for every drive configuration. For the introduced drive design the copper losses amount to $8\,\mathrm{W}$, showing a good agreement with the in vitro validation. Additional losses of the inverter and the lead cables are not included. Further, the current weight of the drive unit and the complete TAH amount to $517\,\mathrm{g}$ and $923\,\mathrm{g}$ respectively. When comparing to the weight of the human heart, which is about $400\,\mathrm{g}$, the TAH is obviously too heavy. Therefore the dimensions of the device have to be reduced, yielding higher losses.

Although initial in-vivo test verified the TAH and therefore the drive concept, the desired durability of five years is not proven yet. Import factors are a validation of the biocompatability of the housing material as well as no failure of any pump or drive component such as the blood chamber diaphragm or the springs, realizing the power transfer to the mover.

References

[1] World-Health-Organization, "http://www.who.int/mediacentre/factsheets/," accessed in November 2010.

[2] J. G. Copeland, R. Smith, F. Arabia, P. E. Nolan, G. K. Sethi, P. H. Tsau, D. McClellan, and M. J. Slepian, "Cardiac replacement with a total artificial heart as a bridge to transplantation," *N Engl J Med*, vol. 351, pp. 859–867, August 2004.

[3] "Abstracts from the 14th congress of the international society for rotary blood pumps," *Artif. Organs*, vol. 30(11), p. A 27, 2006.

[4] H. Miura, S. Arai, Y. Kakubari, F. Sato, H. Matsuki, and T. Sato, "Improvement of the transcutaneous energy transmission system utilizing ferrite cored coils for artificial hearts," *IEEE J MAG*, vol. 42(10), pp. 3578–3580, Oct. 2006.

[5] T. Finocchiaro, T. Butschen, P. Kwant, U. Steinseifer, T. Schmitz-Rode, K. Hameyer, and M. Leßmann, "New linear motor concepts for artificial hearts," *IEEE Transactions on Magnetics*, vol. 44(6), pp. 678–681, 2008.

[6] M. Leßmmann, T. Finocchiaro, U. Steinseifer, T. Schmitz-Rode, and K. Hameyer, "Concepts and designs of life support systems," *IET Science, Measurement & Technology*, vol. 2(6), pp. 499–505, 2008.

[7] A. Pohlmann, M. Leßmann, T. Finocchiaro, U. Steinseifer, T. Schmitz-Rode, and K. Hameyer, "Numerical computation can save life: FEM simulations for the development of artificial hearts," *IEEE Transactions on Magnetics*, 2011. Accepted for publishing.